16 January 1998

ELSEVIER

Chemical Physics Letters 282 (1998) 313–317

CHEMICAL PHYSICS LETTERS

The effect of translational energy on collision-induced dissociation of highly excited NO_2 on MgO(100)

D.W. Arnold [1], M. Korolik, C. Wittig, H. Reisler

Department of Chemistry, University of Southern California, Los Angeles, CA 90089-0482, USA

Received 8 September 1997

Abstract

Collision-induced dissociation of highly excited NO_2 (i.e., mixed $^2B_2/^2A_1$ molecular eigenstates just below D_0) impinging on MgO(100) surfaces has been studied as a function of NO_2 internal excitation at an incident translational energy of 4400 cm^{-1} by using state-selective NO detection. NO internal energy distributions as well as the average energy transferred per activating collision have been obtained. The results, in particular the NO $[^2\Pi_{1/2}]/[^2\Pi_{3/2}]$ population ratios, indicate the presence of exit-channel interactions with the surface that are dependent on collision energy. © 1998 Elsevier Science B.V.

1. Introduction

Experimental studies of collision-induced dissociation (CID) at well-defined hyperthermal energies and with state-selective product detection have provided insight into energy transfer mechanisms and their dependence on environment [1–7]. A recent refinement — the optical preparation of molecules with selected amounts of internal excitation at specified hyperthermal energies — has enabled studies of CID to be carried out at internal energies near the dissociation threshold (D_0), in which case only a small amount of energy needs to be converted from translation to vibration (T → V) to effect CID [1–4]. In these studies, both the incident translational energy, E_{inc}, and the internal energy of the molecules can be varied independently, the former by changing the supersonic expansion conditions and the latter by varying the excitation laser wavelength. Such experiments shed light on the survival probability of highly excited molecules near surfaces, and they are relevant to reverse processes, e.g., can products of surface reactions leave the surface in excited states?

The CID of internally excited NO_2 (hereafter denoted NO_2^*) has been studied previously in the gas phase [2–4] and with crystalline surfaces [1]. In those experiments, hyperthermal NO_2 in a molecular beam was excited to mixed $^2B_2/^2A_1$ molecular eigenstates near D_0 by using laser excitation, and the NO product was detected state-selectively. The gas-phase results have led to the suggestion that CID involves two largely independent steps: collisional activation followed by unimolecular decomposition. During the decomposition step, the gaseous 'collider' (i.e., the species colliding with NO_2) is at a large enough distance (on average) to minimize sec-

[1] Present address: Sandia National Laboratory, Mail Stop 9671, Livermore, CA 94551-0969, USA.

PII S0009-2614(97)01277-3

ondary interactions with the excited NO_2 or its fragments.

Studies of NO_2^* colliding with MgO(100) surfaces at $E_{inc} = 1940\ cm^{-1}$ have shown subtle differences with gas-phase CID, especially in the internal excitations of the NO fragment [1]. In this Letter, we report additional studies of the CID of NO_2^* on MgO(100) aimed at understanding the molecule–surface CID mechanism and how it differs from the gas-phase CID mechanism. We argue that in the molecule–surface case the collisionally activated NO_2 and/or its fragments experience significant interactions with the MgO(100) surface (which depend on E_{inc}), and that this is the main source of the observed differences.

2. Experimental details

The experiments were carried out in a UHV apparatus that has been described in detail elsewhere [1,5–7]. Pulsed supersonic expansion of an NO_2/O_2 mixture (with $[NO_2]/[O_2] \sim 1$) seeded in He produces a molecular beam of cold NO_2 whose translational energy is controlled by changing the seed ratio of the gas mixture. In the present work $E_{inc} = 4400\ cm^{-1}$ was employed, and the incident angle was $\Theta_{inc} = 15°$. The rotational temperature of NO_2 in the beam (estimated from the rotational temperature of the background $NO(^2\Pi_{1/2})$ which is always present in NO_2 samples) is ≤ 10 K. The gas pulse (150–200 μs) is skimmed and collimated before entering the UHV chamber ($\sim 10^{-10}$ Torr), where collisions occur with an ex situ cleaved MgO(100) surface. The crystal is treated by heating in O_2 as described previously [1], and its quality is checked by He diffraction and Auger spectroscopy. A surface temperature of 300 K is maintained in these experiments.

Jet-cooled NO_2 is excited into the mixed $^2B_2/^2A_1$ manifold of eigenstates at ~ 400 nm, by using the output of an excimer laser pumped dye laser (0.4 cm^{-1} linewidth, 3–4 mJ). The laser beam, collimated to a 2 mm width along the molecular beam axis with a cylindrical lens, excites the molecules ~ 20 mm from the MgO surface. A 14–20 μs pump–probe delay allows the NO_2^* to collide with the surface and the resulting CID products to reach the detection region. The relatively long fluorescence lifetime of NO_2^* (~ 50 μs) [8] ensures that a significant fraction of the molecules remains in the excited state upon arrival at the surface. NO fragments are detected state-selectively 3–5 mm from the surface by 1 + 1 (226 nm + 280 nm) REMPI via the $A^2\Sigma^+ \leftarrow X^2\Pi$ transition as described before [5–7]. The probe beams are produced by a dye laser whose doubled output (~ 280 nm) is Raman shifted to ~ 226 nm. After ionization, NO^+ is detected with a bare channeltron. The probe beams propagate parallel to the surface, and angular distributions are obtained by measuring the NO signal along an arc around the collision center.

Several competing processes and background signals must be accounted for in the data analysis, the most important arising from the background NO in the NO_2 beam [3]. Expansion-cooling ensures that only the lowest $NO(^2\Pi_{1/2})$ rotational levels have significant populations; nonetheless, collisions excite background NO from low J into higher rotational states [9], necessitating corrections to the monitored NO signal. Background signals of different origins are singled out by operating the pump laser in *on/off* sequences, and they are subtracted from the total signal for each data acquisition cycle, thereby minimizing errors due to long-term drifts. Data processing also includes normalization by the pump and probe pulse energies.

3. Results

Key to the success of these experiments is that CID occurs only with NO_2^*; ground-state NO_2 cannot acquire sufficient energy via the collision to dissociate. Thus, CID occurs only at excitation wavelengths that coincide with NO_2 absorption features, as illustrated in Fig. 1. Fig. 1a displays the laser-induced fluorescence (LIF) spectrum of NO_2 near D_0; the spectrum is congested, but exhibits distinct, narrow bands. In Fig. 1b, the corresponding CID yield spectrum, obtained by monitoring $NO(^2\Pi_{1/2}, J = 5.5)$ and corrected to account for spurious signals as described before [1,2], is shown. The upper scale ($D_0 - h\nu$) indicates the $T \rightarrow V(NO_2)$ energy re-

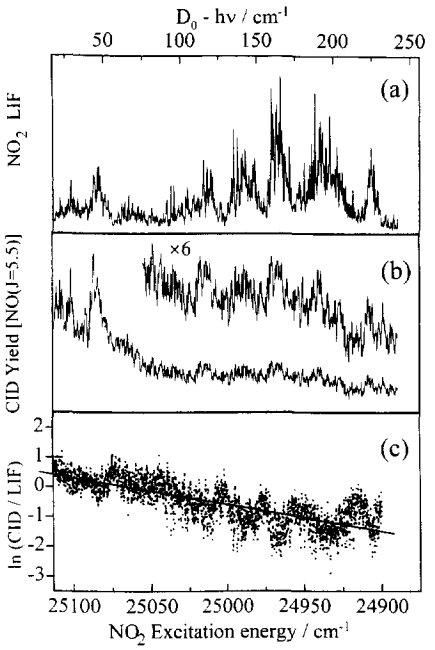

Fig. 1. Jet-cooled NO_2 LIF excitation spectrum. (b) $NO(^2\Pi_{1/2}; v=0; J=5.5)$ CID yield as a function of NO_2^* excitation energy ($h\nu$) at $E_{inc}=4400\ cm^{-1}$. (c) Semilog plot of the point-by-point ratio of the CID and LIF spectra. The top axis indicates energy below D_0.

quired to effect dissociation. The correspondence between the peak positions in the two spectra is evident. Closer inspection, especially in the region of small $D_0 - h\nu$, where the CID signal is largest,

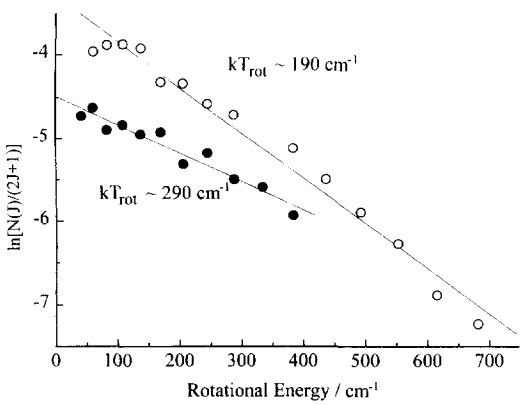

Fig. 2. Boltzmann plots of NO ($v=0$) $^2\Pi_{1/2}$ and $^2\Pi_{3/2}$ rotational populations measured at a fixed NO_2 excitation energy of $D_0 - h\nu = 41\ cm^{-1}$. Open and filled circles display the populations of the $Q_{11}+P_{21}$ and $Q_{22}+R_{12}$ lines, respectively.

reveals that even the finer features in the LIF spectra are reproduced in the CID yield spectrum. Also, as in previous cases [3,4], the CID yield signal decreases rapidly as the required $T \rightarrow V$ energy increases.

A measure of the average energy transferred per activating collision, $\langle \Delta E \rangle$, can be obtained from the semilog plot of the point-by-point ratio of the CID yield spectrum and the LIF spectrum. The higher $T \rightarrow V(NO_2)$ efficiency expected for the higher E_{inc} of the present experiment, combined with higher detection sensitivity, enable $\langle \Delta E \rangle$ to be obtained for the first time in gas-surface CID of NO_2^*. [2] The linear dependence (on average) of $\ln(I_{CID}/I_{LIF})$ on excitation energy implies that the fraction of NO_2^* molecules that undergoes CID decreases exponentially with increasing energy deficiency according to:

$$I_{CID} \propto I_{LIF} \exp\left[-(D_0 - h\nu)/\langle \Delta E \rangle\right]. \quad (1)$$

Such behavior is common in gas-phase energy transfer — the phenomenological exponential gap law [10]. A linear least-squares fit in the range $17\ cm^{-1} \leq (D_0 - h\nu) \leq 240\ cm^{-1}$ gives $\langle \Delta E \rangle = 115 \pm 35\ cm^{-1}$. [3] As with $E_{inc} = 1940\ cm^{-1}$, the CID yield signal peaks near the specular scattering angle.

NO rotational and spin–orbit distributions are obtained by setting the excitation laser frequency at a prominent absorption peak and scanning the probe laser. Fig. 2 displays the rotational distributions obtained by using the $Q_{11}+P_{21}$ and $Q_{22}+R_{12}$ lines originating from the $^2\Pi_{1/2}$ and $^2\Pi_{3/2}$ states, respectively, and obtained at $D_0 - h\nu = 42\ cm^{-1}$ ($h\nu = 398.57$ nm). Similar distributions are obtained for other rotational lines within each spin–orbit state, and also at excitation energies 137 and 157 cm^{-1} below D_0. Since the distributions appear Boltzmann-like, they are characterized by parameters T_{rot} obtained from the slopes of semilog plots such as those shown in Fig. 2; the kT_{rot} values are $190 \pm 40\ cm^{-1}$ and $290 \pm 60\ cm^{-1}$ for the $^2\Pi_{1/2}$ and

[2] The fraction of the excited molecules whose fluorescence is detected does not vary significantly throughout the narrow excitation region employed here.

[3] We exclude the region $D_0 - h\nu = 0$–$17\ cm^{-1}$ from the fit, as it is dominated by photodissociation of rotationally excited NO_2 in the beam [3,4].

$^2\Pi_{3/2}$ states, respectively. These values are comparable to, or slightly lower than, those obtained in scattering from MgO(100) at 1940 cm^{-1} [1] and with gas-phase colliders [3,4].

By summing the populations of all rotational levels in each NO spin–orbit state, the ratio $[^2\Pi_{1/2}]/[^2\Pi_{3/2}] \sim 0.4 \pm 0.05$ is obtained. This value lies between the unity ratio obtained in molecule–surface CID at $E_{inc} = 1940$ cm^{-1} [1] and the ratios obtained in the gas-phase experiments [3,4]. It is also slightly higher than the ratio of approximately 0.3 obtained in the unimolecular decomposition of NO_2 at excess energy ~ 2000 cm^{-1} [11].

4. Discussion

The present results, taken together with the gas-phase CID studies [2–4] and the molecule–surface CID results obtained at $E_{inc} = 1940$ cm^{-1} [1], enable us to obtain a more complete (albeit still qualitative) picture of the reaction mechanism. It is therefore useful to summarize the previous studies.

Gas-phase CID can be described as a two-step process: (1) collisional activation creates a distribution of excited NO_2 levels above D_0 and (2) subsequent unimolecular decomposition yields NO + O. The collider plays mostly a spectator role, and a statistical model, based on the assumption that the fractional population of NO_2 above D_0 decreases exponentially with increasing energy, reproduces the experimental observations rather well [3]. Indications of minor exit-channel interactions with the collider are revealed mainly through the dependence of the NO spin–orbit ratio on the nature of the collider. The average energy transferred per collision depends on the stiffness of the collision partner, with Ar exhibiting the largest $\langle \Delta E \rangle$ values, while polyatomic colliders give smaller values. As expected, $\langle \Delta E \rangle$ increases with E_{inc}, as do the rotational and spin–orbit excitations of the NO product.

The molecule–surface results reveal some intriguing differences: (i) the amount of energy transferred per collision is smaller than in the gas phase; (ii) rotational excitation does not increase (and may even decrease) with increasing E_{inc}; and (iii) the NO spin–orbit population ratios are different than in both gas-phase CID and collisionless unimolecular decomposition, and depend on E_{inc}. These differences suggest that product state distributions are influenced by exit channel interactions between the decomposing NO_2 and/or its fragments with the surface.

From the many studies of photoinitiated unimolecular decomposition of gaseous NO_2, a robust signature has emerged: the $[^2\Pi_{3/2}]/[^2\Pi_{1/2}]$ ratio of the NO product is always smaller than the statistical value of unity [11,12]. This propensity is also present in gas phase CID with small collision partners (e.g., Ar) [3], and is in qualitative agreement with the picture of collisional activation followed by unimolecular decomposition. However, when CID deviates from the separable, two-step process described above, significant interactions between the collision partner and the CID products can affect energy partitioning, resulting, for example in more 'equilibrated' NO spin–orbit populations [3,4].

Exit-channel interactions are more complex in the molecule–surface CID of NO_2^* than in gas-phase CID. Molecule–surface binding energies of the parent (and its fragments) are significant, and energy transfer to the surface may be substantial. In addition, molecule–surface forces are likely to be stronger and longer-range for highly excited molecules than for unexcited molecules. Thus, one cannot assume a priori that decomposition following collision with MgO proceeds in a way that parallels gas phase CID. Measurements at different collision energies reveal the influence of molecule–surface exit channel interactions on the state distributions of the NO product.

It is probable that some fraction of the NO will interact strongly with the surface, since its binding energy is ~ 0.2 eV [14]. For example, suppose some of the post-collision NO_2 molecules rebound from the surface with speeds ~ 6 Å/ps, and recall that the NO_2 collision-free unimolecular decomposition rate several hundred cm^{-1} above D_0 is $\sim 10^{12}$ s^{-1} [13]. In this case, *some* decomposition occurs before the parent and fragments are free from the surface. Moreover, studies of expansion-cooled NO scattering from MgO(100) have shown that the $[^2\Pi_{3/2}]/[^2\Pi_{1/2}]$ ratio for the scattered NO is near the statistical value of unity [15]. This is similar to the value obtained in NO_2^* CID on MgO(100) at $E_{inc} = 1940$ cm^{-1}, but in contrast to the lower value

(0.3) obtained in photoinitiated NO_2 unimolecular decomposition [11,12].

The observed product state distributions reported here for the higher E_{inc} value of 4400 cm^{-1} is consistent with this picture. The similarity of the spin–orbit ratio (0.4) to the unimolecular decomposition value (0.3) suggests that at this higher collision energy the dissociating NO_2 molecules escape from the surface prior to decomposition. Clearly the extent of secondary interactions with the surface depends on E_{inc}. It should be kept in mind that the present experiments detect only those NO_2^* molecules whose internal energy exceeds D_0 following $T \rightarrow V(NO_2)$ and subsequent interactions with the surface. Given the smallness of the signals, this fraction is expected to be modest. Note that the peaking of the NO signal near the specular angle means that the dissociating molecules retain some memory of the momentum of the incident NO_2^*; i.e., trapping–desorption, if it occurs at all, is a minor channel.

The value of $\langle \Delta E \rangle$ obtained at $E_{inc} = 4400$ cm^{-1} is lower than the values obtained with gas phase colliders at about half this energy. For example, $\langle \Delta E \rangle$ values range from 135 cm^{-1} for NH_3 to 307 cm^{-1} for Ar [3,4], pointing again to the significant role played by energy transfer to the surface in the molecule–surface collisions. In contrast to gas-phase CID, where the NO internal excitation increases with E_{inc}, not only are the spin–orbit populations colder at higher E_{inc}, but the rotational excitation of the NO product does not increase, and perhaps even decreases slightly, at higher E_{inc}. This again reflects the subtle influence of interactions with the surface and their dependence on E_{inc}. Thus, all of the evidence collected to date is consistent with a dissociation mechanism in which NO_2^* gains energy in the collision and some of these molecules decompose before they can free themselves from the environs of the surface.

Acknowledgements

This research was supported by the US Air Force Office of Scientific Research. The authors thank K. Mikhaylichenko for obtaining the NO_2 LIF spectrum and Andrei Sanov for stimulating discussions.

References

[1] H. Ferkel, J.T. Singleton, H. Reisler, C. Wittig, Chem. Phys. Lett. 221 (1994) 447.
[2] C.R. Bieler, A. Sanov, M. Hunter, H. Reisler, J. Phys. Chem. 98 (1994) 1058.
[3] A. Sanov, C.R. Bieler, H. Reisler, J. Phys. Chem. 99 (1995) 7339.
[4] C.R. Bieler, A. Sanov, C. Capellos, H. Reisler, J. Phys. Chem. 100 (1996) 3882.
[5] E. Kolodney, D. Baugh, P.S. Powers, H. Reisler, C. Wittig, J. Chem. Phys. 90 (1989) 3883.
[6] E. Kolodney, P.S. Powers, L. Hodgson, H. Reisler, C. Wittig, J. Chem. Phys. 94 (1991) 2330.
[7] P.S. Powers, E. Kolodney, L. Hodgson, G. Ziegler, H. Reisler, C. Wittig, J. Phys. Chem. 95 (1991) 8387.
[8] K.O. Patten Jr., J.D. Burley, H.S. Johnston, J. Phys. Chem. 94 (1990) 7960.
[9] C.R. Bieler, A. Sanov, H. Reisler, Chem. Phys. Lett. 235 (1995) 175.
[10] J. Troe, J. Chem. Phys. 66 (1977) 4745.
[11] M. Hunter, S.A. Reid, D.C. Robie, H. Reisler, J. Chem. Phys. 99 (1993) 1093.
[12] S.A. Reid, D.C. Robie, H. Reisler, J. Chem. Phys. 100 (1994) 4256.
[13] S.I. Ionov, G.A. Brucker, C. Jaques, Y. Chen, C. Wittig, J. Chem. Phys. 99 (1993) 3420.
[14] H. Ferkel, L. Hodgson, J. Singleton, P. Blass, H. Reisler, C. Wittig, J. Chem. Phys. 100 (1994) 9228.
[15] E. Kolodney, D. Baugh, P.S. Powers, H. Reisler, C. Wittig, Chem. Phys. Lett. 145 (1988) 177.